UNIVERSITY OF OKLAHOMA

GRADUATE COLLEGE

EFFECTS OF PH ON THE RAMAN SPECTRA OF BRINES

A THESIS

SUBMITTED TO THE GRADUATE FACULTY

in partial fulfillment of the requirements for the

Degree of

MASTER OF SCIENCE

By

BAILEY ABNEY
Norman, Oklahoma
2022

EFFECTS OF PH ON THE RAMAN SPECTRA OF BRINES

A THESIS APPROVED FOR THE
SCHOOL OF GEOSCIENCES

BY THE COMMITTEE CONSISTING OF

Dr. Megan Elwood Madden, Chair

Dr. Gerilyn Soreghan

Dr. Shannon Dulin

Table of Contents

Abstract

The use of Raman spectroscopy on Mars can help us understand the geochemistry of past or present brines on Mars which could help us assess the overall habitability of Mars. Raman can detect biosignatures from organic matter, look for signs of transient flowing water, analyze fluid inclusions and measure ion concentrations in solution. While Raman can be used to determine the bulk composition of a brine it is essential to understand what other factors may also affect the Raman spectra. We conducted experiments assessing the effects of pH on the Raman spectra of Mars analog brines. Our results show Raman spectra of carbonate, sulfate, and phosphate-bearing solutions vary considerably with pH, while chloride and perchlorate brines recorded only minor or no changes with pH. We found that changes in pH correspond to changes in concentration for various species which in turn affects peak intensity. By plotting peak heights against pH for certain brine types we should be able to determine the relative pH of an unknown brine of similar composition. We also found that shifts in peak position occur as pH changes, likely due to the presence of different species at different pH conditions. Changes in the spectra represent changes in the overall aqueous chemistry of the solution which can affect habitability and biogeochemical processes.

Introduction

Raman spectroscopy is an important tool that can be used to determine the chemistry of geomaterials, including brines and other natural waters on Earth or other planets such as Mars. Brines may be important fluids on planetary bodies due to their low freezing points and vapor pressures (Clark and Van Hart, 1981). Despite their likely importance, brines are often difficult to analyze due to their relatively high viscosities/densities which can clog traditional aqueous analytical tools and high solute concentrations can overwhelm the detectors leading to poor readings (McGraw et al., 2018). Raman spectroscopy can analyze brines without physical contact with the sample, preventing contamination, corrosion, and staying within planetary protocols. Raman uses a laser to excite the sample and a spectrometer to collect the Raman shifted light to help determine the molecular composition of the sample (McGraw et al., 2018). Raman spectroscopy can also be used to analyze fluid inclusions trapped inside ancient rocks or minerals (Benison et al., 1998). These fluid inclusions can be used to determine the water chemistry and relative pH levels of water in the past which has significant implications for scientists trying to unravel the history of Earth or even other planets such as Mars. In the case of Mars, Raman spectroscopy could help determine whether or not Mars was habitable in the past and if not, why (Uckert et al., 2021)? Being able to understand the geologic history of Mars and its habitability are also pertinent for future efforts to send humans to Mars. This is why the Perseverance Rover, that recently made a successful landing on Mars, was equipped with a Raman spectrometer, SHERLOC (Scanning Habitable Environments with Raman and Luminescence for Organics and Chemicals) to help assess the geologic history of Martian surface conditions and search for organic molecules that may be indicative of past life (Uckert et al., 2021).

Various data suggest that Mars used to have a hydrologic cycle much like Earth's; for example, sedimentological evidence of alluvial-fan and groundwater-fed crater-lake systems, as well as mineralogical evidence such as the detection of hydrothermal phases like serpentine and phyllosilicates (Michalski et al., 2013). The Mars Advanced Radar for Subsurface and Ionosphere Sounding (MARSIS) recently detected signs of liquid water near the Martian south pole beneath the ice caps (Lauro et al., 2021). It's hypothesized that this water consists of some form of a hypersaline brine such as a perchlorate brine capable of remaining metastable for extended periods of time below eutectic temperatures (Lauro et al., 2021). Since we cannot yet study these subsurface brines however, we must look to the surface for current signs of flowing water or other clues that could help us determine the habitability of Mars. Using Raman spectroscopy to measure ions in solution within fluid inclusions and studying their peak height ratios can help us understand the geochemical conditions on Mars millions or even billions of years ago (McGraw et al., 2018). Raman spectroscopy can also be used to search for current signs of transient flowing water on the Martian surface, such as hydrated salts or the detection of liquid water absorptions, occurring along recurring slope lineae (RSL) during the warmer seasons (Ojha et al., 2015). Future rovers will likely investigate equator-facing slopes with low albedo, that absorb more sunlight radiation in search for brines penetrating the surface, creating these RSL structures (McEwen et al., 2013). While searching for transient flows other areas of interest will likely include ancient crater lakes, deltas, or outcrops with course grained material

that is more likely to have a brine permeate through to the surface. Regions with high concentrations of salt will likely be another area of interest as deliquescence is more likely to occur.

Furthermore, Raman is able to detect trace amounts of organic matter and determine, based on distribution/concentration factors, if these organic molecule accumulations are likely biosignatures or simply background abiotic noise (Sapers et al., 2019).The detection of transient brines in combination with signatures of organic matter on the Martian surface would have significant implications for the future habitability of Mars. Quantitative studies using Raman spectroscopy to measure solute concentrations in brines have been previously demonstrated by comparing anion peaks with O-H bending water peaks near 1640 cm^{-1}, but further work is needed to see how temperature and pH affects the spectra (McGraw et al., 2018). By analyzing how pH affects peak height ratios and peak positions for known brines in the lab, we can compare those laboratory measurements to future Mars data transmitted back from the Perseverance Rover to help determine the chemical composition and relative pH of past brines on Mars.

Previous studies used Raman spectroscopy to measure sulfate and perchlorate concentrations by comparing anion peaks with the O-H water peak at 1640 cm^{-1} in Na_2SO_4 and $NaClO_4$ solutions (McGraw et al., 2018). Sulfate and perchlorate brines are of particular interest to planetary scientists because they represent likely endmember brines on habitable planetary bodies such as Europa, Enceladus, Ceres, and Mars. Furthermore, perchlorate and sulfate salts have already been detected on Mars and may offer valuable information pertaining to the geochemistry and habitability of ancient or modern brines on Mars (Ojha et al., 2015). Results of the study showed that increases in standard concentration lead to increases in peak height for the sulfate and perchlorate peaks while the water peak at 1640 cm^{-1} saw a decrease in relative intensity (McGraw et al., 2018). Another study focused on the effects monovalent cations (K^+, Na^+, NH_4^+) and hydration have on the position of Raman peaks for the various vibrational frequencies of the sulfate anion (Mabrouk et al., 2013). In solid sulfate salts, Raman peaks shift towards lower wavenumbers with an increase in the ionic radius of the corresponding cations, but in the aqueous sulfate solutions cation size imparts no effect on peak positions. Additionally, hydration of the sulfate salts causes a slight shift towards lower wavenumbers and a broadening of all sulfate peaks (Mabrouk et al., 2013).

Previous studies of Raman spectral data showed signs of unexpectedly low pH, acidic groundwater systems in Earth's deep-time sedimentary record (Benison et al., 1998). Permian red beds deposited in the North American midcontinent were previously believed to originate from alkaline mudflats and non-marine saline lakes. However, Raman analysis of fluid inclusions trapped inside halite crystals sampled from Kansas and North Dakota suggest that these groundwater systems were highly acidic, changing scientists' perception of North America during the Permian and forcing scientists to re-evaluate the reconstruction of Earth's climates and groundwater systems during this time (Benison et al., 1998). Many of these ancient, acidic Earth systems are posited to be analogous to past brines on Mars or even to groundwater systems beneath the modern Martian surface. Studying these systems via Raman spectroscopy is

important, in preparation for future Mars exploration and data analysis (Benison et al., 1998). The pH of a solution affects HSO_4^-: SO_4^{2-} ratios and is driven by the overall bulk chemistry of the solution. The fluid inclusions from the Permian red beds exhibit a pattern within the spectral data concerning the bisulfate-sulfate ratio. For a pH < 0 there were two HSO_4^- peaks present in the spectra while the solutions with a pH between 0 and 1 show only one peak. When the pH was ≥ 1 then no HSO_4^- peaks appeared. So, if one or two HSO_4^- peaks occur, then the Raman spectra indicates that the relative measure of pH is highly acidic in sulfate solutions (Benison et al., 1998). These observations from the Permian red beds could similarly be applied on Mars to determine the relative pH levels of past brines through the use of trapped fluids in minerals.

Based on observations of jarosite found at Meridiani Planum and other regions, researchers have hypothesized fairly acidic ephemeral fluids flowed along the surface of Mars in its past (Squyres et al., 2004). On Earth jarosite commonly forms through precipitation from acidic lakes or through aqueous oxidation of iron-sulfide minerals in acid mine drainage systems (Benison and Goldstein, 2002). When pH exceeds 2.5 jarosite becomes metastable and breaks down to form iron oxides which have also been observed in close proximity to jarosite at Meridiani Planum, suggesting the rocks in this region underwent a period of aqueous diagenesis post jarosite formation (Elwood Madden et al., 2012). Additionally, evidence from Gale crater indicates there was a lake system present on Mars fed by alluvial runoff approximately 3.1-3.8 Ga (Hurowitz et al., 2017). Mineralogical and geochemical evidence obtained from the Murray formation within Gale crater suggest that this was a redox stratified lake with pH ranging from neutral to alkaline (Hurowitz et al., 2017). While exploring Gale crater, the Curiosity rover detected nitrogen, organic carbon compounds, phosphate minerals, as well as sulfur and iron-bearing minerals in various redox states within the sedimentary strata suggesting that the physical/chemical conditions needed to establish a habitable environment existed on Mars 3.1-3.8 Ga (Hurowitz et al., 2017).

So, while there is strong evidence of rather acidic fluids traversing the Martian surface billions of years ago there is also evidence for lakes of neutral or alkaline chemistries conducive to life that occupied impact craters (Hurowitz et al., 2017). Determining the pH of past fluids on Mars is important because it reveals the tolerances of potential life forms that could have existed in the past and gives us insight on what bacterial life forms could be thriving beneath the Martian surface in underground aquifers. If the pH is too acidic only certain prokaryotes known as extremophiles could have survived. More neutral waters could have led to a larger variety of chemoautotrophs and thermophiles which could still be thriving in the subsurface, taking advantage of serpentinization reactions (Michalski et al., 2013).

Furthermore, if humans are to tap into these subsurface aquifers in the future, pH will play a role in the survival of future explorers as water is an essential resource. In this study, we aim to see how pH can affect the peak intensities and peak positions of anions within Raman spectra. These shifts in the peaks represent changes in the overall aqueous chemistry of the water which can have major effects on habitability and biogeochemical processes. Our goal is to create a library or database of Raman spectra for various brine types along with corresponding pH values for each lab sample to compare with future Raman data collected on Mars in hopes to

determine what we are seeing on the Martian surface and if it is or ever was a habitable environment.

Methods

We created aqueous solutions of sulfate, carbonate, phosphate, chloride, chlorate, and perchlorate anions over a range of pH conditions by mixing anion standards with buffer solutions of known pH in 1:1 mixtures. Cations used in the experiment included hydrogen, sodium, and magnesium. Our study focused on brines that could have existed on Mars throughout its geologic past, including $CaCl_2$, NaCl, $MgSO_4$, $NaNO_3$, Na_2SO_4, $MgCl_2$, $NaHCO_3$, Na_2CO_3, $NaHSO_4$, NH_4Cl, NaF, $NaClO_4$, $NaClO_3$, NaH_2PO_4, Na_2HPO_4, H_3PO_4. We used both HCl (pH ~0-5) and NaOH (pH ~8-13) solutions to adjust the pH and measured the pH of a separate aliquot of each solution using an Orion pH electrode. We created five stock HCl solutions of known pH (1-5) by adding drops of 6N HCl to 200 ml of ultra-pure water (UPW) (Table 1). We also used the undiluted 6N HCl as an additional pH buffer (pH=0.1), yielding 6 acidic pH standard solutions that we mixed with our brine standards. We measured 20 ml of each pH standard solution in a graduated cylinder and then poured it into a 60 ml plastic bottle for storage, labeling them as we went. Then we added 20 ml of 1M brine standard and mixed it with the pH standard, yielding 40 ml of pH adjusted brine standard for analysis. We repeated this process for all 16 brines and UPW as a control, yielding a total of 102 (17*6) acidic-brine mixtures (Table 1). We mixed each solution thoroughly before recording the pH values using the pH electrode.

We repeated the process using 1M NaOH as the standard to create a range of brine standards with pH > 1. We started with a pH 12.98 solution of NaOH that we diluted with UPW and/or adjusted to lower pH using drops of concentrated HCl solution to create basic standards with pH~8-13 (Table 1). Then we used a graduated cylinder to again add 20 ml of each NaOH buffer solution and 20 ml of each brine standard to create six different basic brine standards. We repeated the process with all 16 brines and UPW giving us another 102 buffer-brine mixtures and recorded their final pH values (Table 1).

For the phosphate brines we also conducted a titration experiment by adding drops of HCl at a rate of 2 ml/minute to an initial 40 ml solution of 1 mol/kg NaH_2PO_4 brine and took sub samples during the titration to fill in the pH gaps from the initial mixing experiments. We analyzed each of the pH-adjusted brine standards using a Renishaw InVia High Resolution Raman Spectrometer to collect spectral data with a 532 nm laser and a 1200 1/cm grating to collect Raman spectra from 400-2700 wavenumbers (cm^{-1}). We placed 1 ml of each solution into a small well on a ceramic painter's plate and collected 10s of data 10 times, allowing the Raman to collect 100s of data to increase the signal intensity.

We processed the Raman spectra, using the Wire 4.2 software package, through a series of four steps, then we curve fit the data for further data analysis. First, we had to remove any gamma ray peaks present and then we truncated the spectra to isolate data from 400-2700 wavenumbers (cm^{-1}). Next, we removed the background noise by selecting minima points along the curve and subtracting the baseline. Lastly, we normalized the intensity from 0 to 1 based on the highest observed peak. Then we used Wire 4.2's curve-fitting tool to help determine the peak

heights, areas and positions of our targeted anions.

Results/Discussion

The Raman spectra collected from various solutions show that pH can greatly affect the peak height ratios and peak positions of target anion solutes in some brines. The Raman spectra for the carbonate, sulfate and phosphate brines vary considerably with pH, while the chloride and chlorate brines recorded only minor or no changes with pH. For this study we focused on salts that showed substantial changes in their Raman spectra with respect to pH which included 1M $NaHCO_3$, $MgSO_4$, Na_2HPO_4 and NaH_2PO_4 (Table 1).

Carbonate Brines

The Raman spectra for 1M $NaHCO_3$ mixed with HCl/NaOH showed that pH exerts a profound effect on peak heights and positions, and thus that these measures can be used to help determine relative pH. We found that the ten spectra with pH values between 9 and 11 showed strong peaks for carbonate, bicarbonate, and carbonyl groups while the lowest pH spectra at pH 5.15 scarcely showed any sign of a HCO_3^- peak at 1017 cm^{-1} and showed essentially no sign of the CO_3^{2-} peak at 1064 cm^{-1} (Figure 1). The 5.15 pH spectrum was also missing a symmetric stretching CO_2 peak at 1360 cm^{-1} that appeared in the more alkaline samples (Rudolph et al., 2007). On the other hand, the highest pH spectra with pH 13.35 showed no signs of a HCO_3^- peak at 1017 cm^{-1} or a CO_2 peak at 1360 cm^{-1} but exhibited the highest CO_3^{2-} peak at 1064 cm^{-1} (Figure 1). These observations correlate well with the speciation diagram for bicarbonate, since the higher the pH, the greater the shift towards a prevalence of carbonate ions (Figure 2). Furthermore, when examining the CO_3^{2-} peak at 1064 cm^{-1} for samples with pH 9-13 we found that the peak decreases as pH decreases and disappears completely in more acidic brines with a $pH \leq 5$ (Figure 1). These observations show how identifying these carbonate peaks and studying their peak height ratios can help determine relative pH levels for a $NaHCO_3$ brine.

Additionally, when looking at the pH 9.23 sample for 1M $NaHCO_3$ mixed with 1M NaOH we found that there was a small mineral peak not present in any of the other samples at 1087 cm^{-1} that we identified as gaylussite ($Na_2(CO3)_2*5H_2O$) (Figure 1). In this case the addition of the NaOH buffer as opposed to the HCl buffer to the $NaHCO_3$ brine likely caused an increase in concentration of sodium and hydroxide that allowed this mineral to form in the lower pH spectra. Since this mineral only formed in the pH 9.23 spectra for 1M $NaHCO_3$ mixed with NaOH it gives a pretty good constraint on relative pH as it does not appear in the next closest pH sample of 9.56. Using the Raman to identify particular mineral peaks that are pH sensitive is another useful method to help determine the relative pH of a brine.

Sulfate Brines

Examination of the spectra collected from the $MgSO_4$ brine mixed with HCl/NaOH at various pH conditions shows the onset of shifts in peak placements or changes in peak intensities with increasing acidity. In figure 3 the peaks around 460, 620, 980 and 1,110 cm^{-1} are all sulfate peaks that correspond to different vibrational modes for the sulfate ion (Sharma et al., 2019). The $v_1(SO_4)$ peak at 980 cm^{-1} represents the symmetric stretching of oxygen atoms in SO_4^{2-}, while the

$v_2(SO_4)$ peak at 460 cm^{-1} corresponds to the symmetric bending of the oxygen molecules within sulfate (Sharma et al., 2019). The $v_3(SO_4)$ peak at 1,110 cm^{-1} and the $v_4(SO_4)$ peak at 620 cm^{-1} correspond to the antisymmetric stretching and antisymmetric bending of the sulfate molecule respectively (Sharma et al., 2019). For the four $MgSO_4$ samples mixed with HCl with a pH between 2.31-8.30 we observed essentially no changes in the peak height ratios or peak positions (Figure 3). However, the Raman spectra for $MgSO_4$ mixed with HCl at a pH of 1.76 and 0.63 exhibit interesting changes in peak positions as well as appearance of additional peaks. The $MgSO_4$ sample at pH 0.63 shows a slight shift to lower wavenumbers for the $v_2(SO_4)$ peak at 460 cm^{-1} and the $v_4(SO_4)$ peak at 620 cm^{-1}. When analyzing the 620 cm^{-1} peak it is also easy to see the $MgSO_4$ sample with pH 1.76 has shifted slightly toward lower wavenumbers as well, just not as much as the more acidic pH 0.63 sample. Furthermore, an additional peak at 1050 cm^{-1} appeared in the pH 0.63 spectra and signs of formation of this peak are evinced by the small hump in the pH=1.76 spectra (Figure 3). Previous work done on symmetric stretching vibrations for sulfate fluid inclusions allowed us to identify the peak at 1050 cm^{-1} as HSO_4^- (Dubessy et al., 1992).

When looking at the speciation diagram for bisulfate it makes sense that only the two $MgSO_4$ samples with a pH < 2 showed signs of a HSO_4^- peak since it has the highest concentration in highly acidic brines (Figure 4). The addition of an HSO_4^- peak along with certain sulfate vibrational mode peaks shifting to lower wavenumbers seem to be clear signs that the $MgSO_4$ brine is highly acidic with a pH ≤ 2. For the $MgSO_4$ brine mixed with 1M NaOH at the six different pH levels there were essentially no noteworthy changes in the Raman spectra as pH varied from 7.24 to 9.42 (Figure 3). This shows us that changes in the spectra for a magnesium sulfate brine are more likely to occur if the pH is highly acidic (pH~2 or less) while pH in more basic $MgSO_4$ brines may be harder to distinguish.

Phosphate Brines

The phosphate brines produced major changes in peak height positions and peak height intensities over the full range of pH conditions investigated, making them a promising indicator of pH in Raman spectra. We found 6 major phosphate peaks corresponding to different vibrational frequencies in NaH_2PO_4 brine that change with pH (Figure 5). The v_1PO_4 peak at 890 cm^{-1} represents a symmetric stretching $P(OH)_3$ bond that can be used to help determine pH (Rudolph et al., 2012). This peak has a high intensity at pH 1.06-5.56, but the peak position shifts to slightly higher wavenumbers in the pH 1.06 sample (Figure 5 and 6). At pH 6-7, the peak intensity decreases, while samples at pH ≥ 7, not only display a significant decrease in intensity but the center of the peak also shifts towards lower wavenumbers and broadens (Figure 5 and 6).

These shifts in peak position likely reflect the different phosphate species present over the pH range contributing to this v_1PO_4 peak. H_3PO_4 is the dominant species in the 1.06 pH sample which could explain the shift towards higher wavenumbers. Then $H_2PO_4^-$ is the dominant species for samples with a pH between 2-7 centered at 890 cm^{-1} and HPO_4^{2-} is dominant in the samples with a pH > 7 which could explain the broadening peak/shift towards lower wavenumbers (Figure 6). The v_2PO_4 peak at 1174 cm^{-1} represents a stretching P=O bond

(Rudolph et al., 2012) that decreases in intensity as pH increases, disappearing completely at pH 5 or more (Figure 5 and 6). This peak likely records H_3PO_4 as this species dominates in very acidic brines and decreases in concentration as pH increases, with no significant concentration expected at pH ≥ 4 (Figure 6).

The v_3PO_4 peak has intensity of ~0.2 in the pH 2.78-5.56 samples, while the pH 1.06 sample has an intensity of ~0.12 and has been shifted towards lower wavenumbers (Figure 6). At pH ≥ 6 the intensity also decreases, but the peak shifts towards higher wavenumbers for samples with pH > 7. This pattern in the direction of peak shift for the v_3PO_4 peak with pH is opposite to the behavior observed in the v_1PO_4 peak. Combining observations between the v_1 and v_3 peaks suggests highly acidic pH causes the v_3PO_4 peak to shift towards lower wavenumbers and the v_1PO_4 peak to shift towards higher wavenumbers while neutral to highly alkaline pH conditions cause the v_3PO_4 peak to shift towards higher wavenumbers and the v_1PO_4 peak to shift towards lower wavenumbers. Both peaks correspond to symmetric $P(OH)_3$ bond structures (Rudolph et al., 2012). However, the bonds for the v_1PO_4 peak are being stretched while the bonds for the v_3PO_4 peak are being bent. This difference in vibration movement could be causing the peaks to shift in opposite directions for highly acidic and basic samples. Furthermore, the phosphate speciation diagram (Figure 6a) suggests the dominant species being observed at the v_3PO_4 peak switches from H_3PO_4 to $H_2PO_4^-$ then HPO_4^{2-} and finally PO_4^{3-}, corresponding to samples with pH < 2, pH 2-7, pH 7-12 and pH > 12 respectively. This makes sense because the addition of hydrogen ions is causing a decrease in pH.

The v_4PO_4 peak at 1075 cm^{-1} represents the asymmetric stretching of $P(OH)_3$ (Rudolph et al., 2012). The v_4PO_4 peak has similar intensity at pH between 2.78-5.56, but lower intensity at pH 1.06 and pH ≥ 6 (Figure 5 and 6). This suggests this peak is due to $H_2PO_4^-$ as it is the most common phosphate species at pH 3-6 (Figure 6a). This shows the v_4PO_4 peak height can be greatly reduced under highly acidic or neutral to alkaline conditions (Figure 5 and 6) which provides minimal insight for determination of the relative pH levels of Raman spectra sent back from Mars brines. However, using this information in conjunction with the other peaks can shed light on whether or not the analyzed brine has a high or low pH. In this case, the lack of a v_2PO_4 peak at 1174 cm^{-1} hints at neutral to alkaline waters but when analyzing this sample alone it may be difficult to notice a missing peak and use that as evidence to justify higher pH (Figure 5). However, the v_5PO_4 peak at 988 cm^{-1} corresponds to a symmetric stretching P=O bond and appears only in samples with pH > 5 (Rudolph et al., 2012). This v_5PO_4 peak intensity maximizes at pH 10.35 and peak intensity decreases at both higher and lower pH conditions (Figure 6). The speciation diagram indicates this peak is likely due to HPO_4^{2-} as this species dominates at pH 9-10 (Figure 6a). Additionally, to narrow down whether a solution containing phosphate has a neutral or alkaline pH one can look for a v_6PO_4 peak around 940 cm^{-1} which corresponds to asymmetric stretching of the $P(OH)_2$ bond structure (Rudolph et al., 2012) and only appears in the samples with a pH > 10 (Figure 5). The v_6PO_4 peak also increases in intensity as pH increases, hinting at PO_4^{3-} speciation (Figure 6b).

We wanted to analyze two separate phosphate brines since they show the most substantial changes with respect to pH. For the Na_2HPO_4 brine mixed with HCl/NaOH we noticed there

were many similarities between its vibrational phosphate peaks and the phosphate peaks observed in NaH_2PO_4, the brine described above. The v_1PO_4 peak at 980 cm^{-1} for Na_2HPO_4 shows a strong correlation with the v_1PO_4 peak for NaH_2PO_4 as it can again be seen not only shrinking but shifting towards lower wavenumbers as the pH increases (Figures 5 and 7). There is a strong, sharp peak at 980 cm^{-1} for the 1.36 pH sample, but the height of the 6.84 pH sample has been reduced to roughly 0.3 intensity and the peak has been shifted slightly towards lower wavenumbers. The nine samples with a pH between 7.76 and 9.27 have been reduced in height to about 0.2 intensity and shifted even more towards lower wavenumbers with their peaks centered around 860 cm^{-1} (Figure 7). This overall trend continues in the pH 13.32 sample which sees and even greater reduction in peak height and a further shift towards lower wavenumbers which is consistent with the pH > 10 samples from the NaH_2PO_4 brine (Figures 5 and 7). The v_2PO_4 peak only appears in the most acidic sample with a pH of 1.36 which correlates well with the previous phosphate brine since the peak essentially disappears at a pH ≥ 5 (Figures 5 and 7). When looking at the v_3PO_4 peak at 535 cm^{-1} we found the center of the peak for the acidic pH 1.36 sample has been shifted slightly towards lower wavenumbers which also correlates well with the more acidic samples, especially the pH 1.06 sample, from the previous phosphate brine (Figure 5 and 7). Additionally, the pH 13.32 sample shows a slight shift towards higher wavenumbers which is consistent with the pH > 10 samples in the NaH_2PO_4 brine.

When comparing the v_4PO_4 peak at 1080 cm^{-1} with that of the previous phosphate brine we found our initial generalizations held true. The highly acidic pH 1.06 sample has a low intensity of 0.2 while the pH ≥ 6 samples see a reduction in intensity as pH increases (Figures 5 and 7). The most alkaline sample with a pH of 13.32 exhibits a peak shift towards lower wavenumbers and a smaller area. When examining the whole picture (Figures 5 and 7) the v_4PO_4 peak appears to have the highest intensity (~1) at a pH of roughly 2.78-5.56 while more acidic and more alkaline samples exhibit a major reduction of this peak, hinting at $H_2PO_4^-$ speciation (Figure 6a). The v_5PO_4 peak also has an intensity of 1 for the pH values between 7.76 and 9.27 while the peak for the pH 6.84 sample has been reduced to about 0.7 intensity and the acidic pH 1.36 sample shows no peak for v_5PO_4 (Figure 7). When comparing the v_5PO_4 peak between both phosphate samples we found this peak disappears around pH ≤ 5, meaning acidic phosphate brines will not exhibit this peak (Figures 5 and 7). Additionally, the v_5PO_4 peak for the pH 13.32 sample exhibits a major height reduction which corresponds nicely with the previous observation of the NaH_2PO_4 brine that showed this peak decreases as pH increases at pH > 10 (Figures 5 and 7). These results suggest the v_5PO_4 peak has the highest intensity in brines with pH 8-10, is nonexistent if pH ≤ 5 and is reduced in brines with a pH between roughly 5 and 7 or in brines with pH > 10. The 13.32 pH sample has a lone peak labeled v_6PO_4 at 940 cm^{-1} which is a clear indicator that this is a highly alkaline brine rather than an acidic or neutral pH sample that shows no peak at 940 cm^{-1} (Figure 7). This v_6PO_4 peak showing up again in the highly alkaline sample is consistent with the data from the phosphate titration experiment of NaH_2PO_4 that showed this v_6PO_4 peak only appears in samples with a pH > 10 (Figure 5 and 7).

Future Work

Here we demonstrate how Raman spectra vary with changes in pH for 4 of the 16 brines

investigated. We have three more brine samples highlighted in yellow on Table 1 that show substantial changes in peak height ratios and peak positions on the Raman spectra due to changes in pH that could be analyzed in the future to create a wider range of data. The remaining nine brine samples consisting of perchlorate, chlorate, chloride, nitrate, and fluoride brines show only minor changes in peak intensity and essentially no changes in peak position of the Raman spectra and will not be of further focus. For the remaining three samples showing significant spectral changes we plan to analyze how changes in pH affect peak height ratios, which peaks form and how vibrational stretching mode peaks for certain compounds change with respect to pH. We also plan to plot curve fit data, such as peak height ratios or peak area ratios for defining peaks, against pH to see if we can find any trends in the data that would help explain how/why pH affects these spectral characteristics. We hope to find deterministic relative pH markers within the Raman spectra that could be extrapolated to help explain future Mars Raman data and help unravel the history of water/habitability on the Martian surface.

Conclusion

The Perseverance rover can use its Raman instrument, SHERLOC, to help determine the chemical composition of past brines on Mars by analyzing fluid inclusions, as well as potentially analyzing modern brines observed on the surface. However, determining the relative pH of the brines will require careful observations of both peak positions and intensities. Our results show that pH can have a significant effect on the peak positions and peak height ratios of the Raman spectra depending on the type of brine. We found that changes in pH correspond to changes in concentration for the various Raman peaks, which in turn affects the peak intensities. By plotting peak heights against pH for the phosphate brines we should be able to determine the relative pH of an unknown phosphate brine. By applying this method to various brine types, it should be possible to constrain the pH of unknown brines (if the brine type has peaks that vary with pH) once the bulk composition is determined. We hypothesized that shifts in peak position are likely due to the different species present over the pH range. Additionally, we found that certain mineral peaks could be used as relative pH markers since certain minerals only form under very specific pH conditions. Future Raman measurements can be compared to these and other spectral libraries to constrain both the composition and environmental conditions affecting the brine, including pH. These types of observations could reveal whether Mars was likely habitable in the past and if will be suitable for humans in the future. The results of our experiments could be very useful to future Mars exploration as we attempt to unravel the history of water on the Martian surface, throughout its geologic past.

Figures and Tables

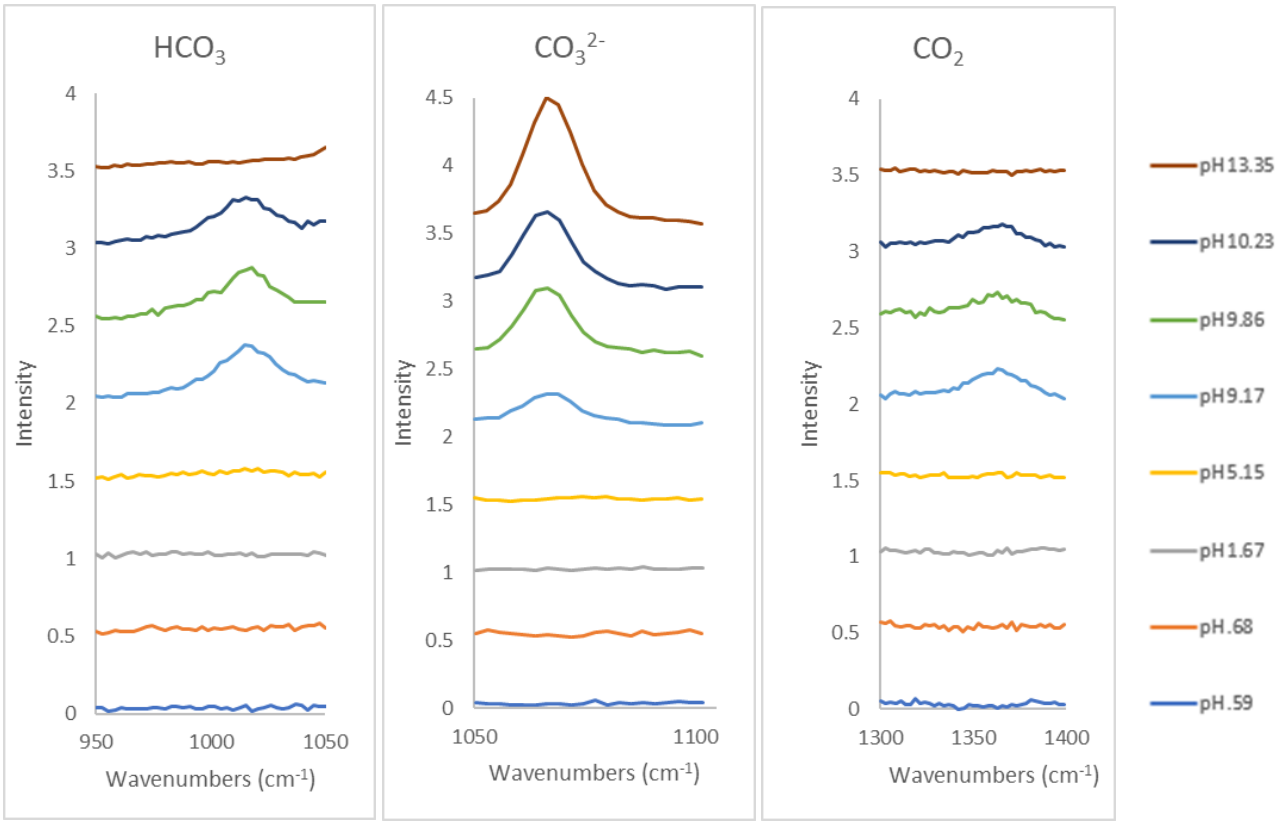

Figure 1) Green laser spectra for 1M $NaHCO_3$ brine mixed with the six different HCl/NaOH buffers at various pH levels (subset of carbonate samples).

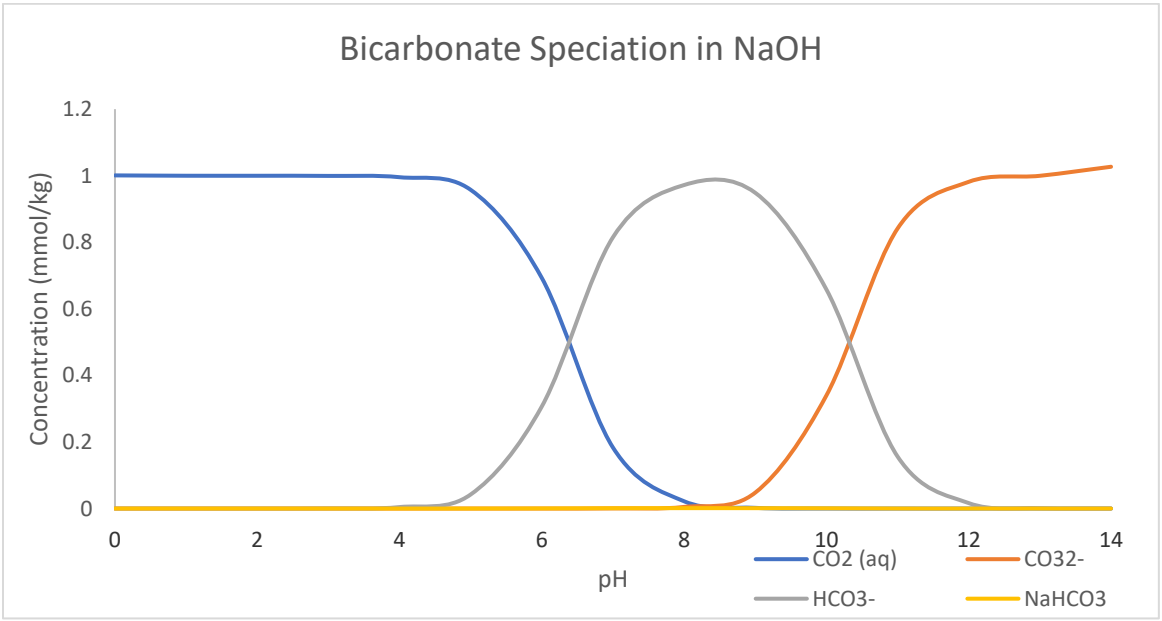

Figure 2) Bicarbonate speciation diagram as predicted by Geochemist's Workbench.

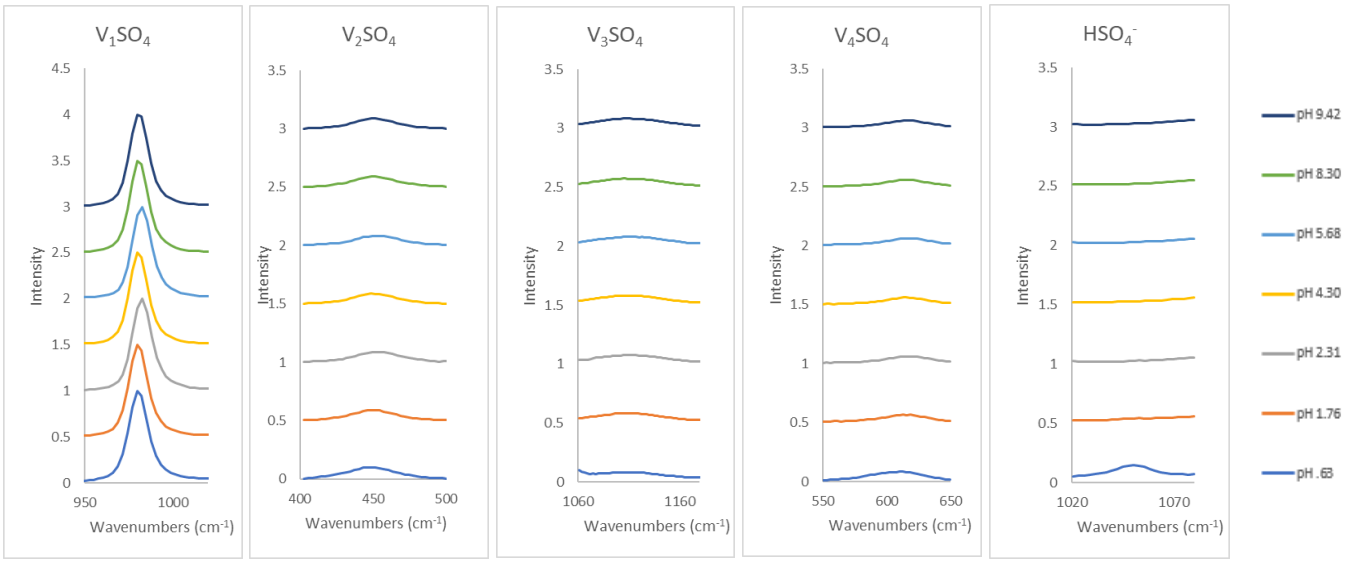

Figure 3) Green laser spectra for $MgSO_4$ brine mixed with the six different HCl/NaOH buffers at various pH levels. Key: v_1: $v_s(SO_4)$; v_2: $\delta_s(SO_4)$; v_3: $v_{as}(SO_4)$; v_4: $\delta_{as}(SO_4)$ (v=stretching, δ=bending, s=symmetric, as=asymmetric). (subset of magnesium sulfate samples)

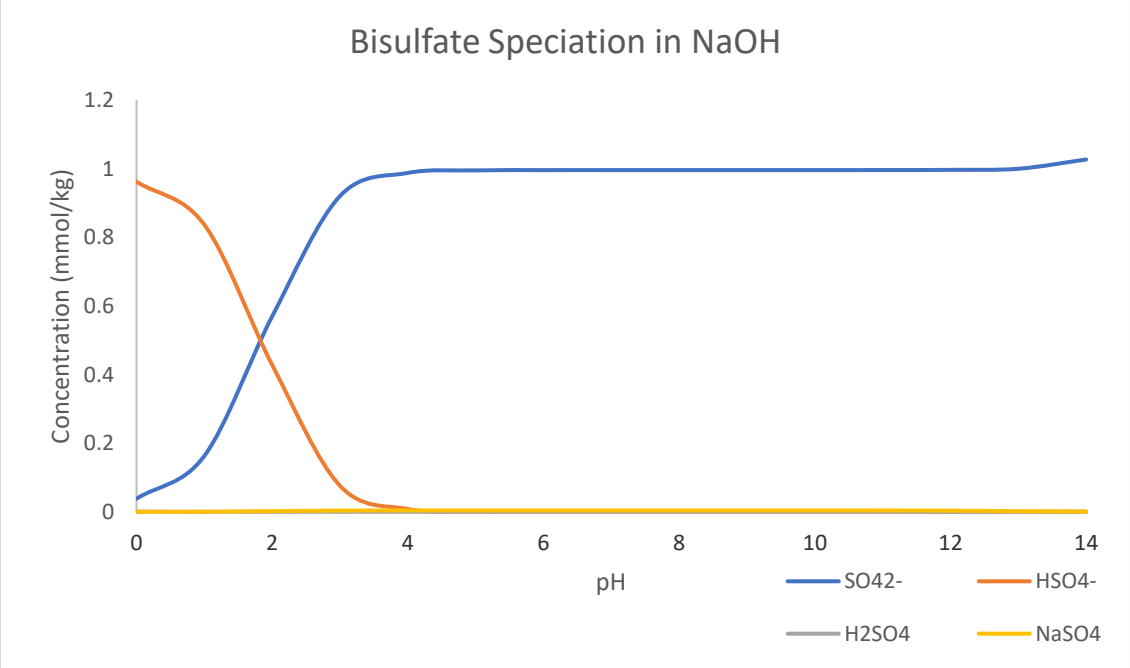

Figure 4) Bisulfate speciation diagram as predicted by Geochemist's Workbench.

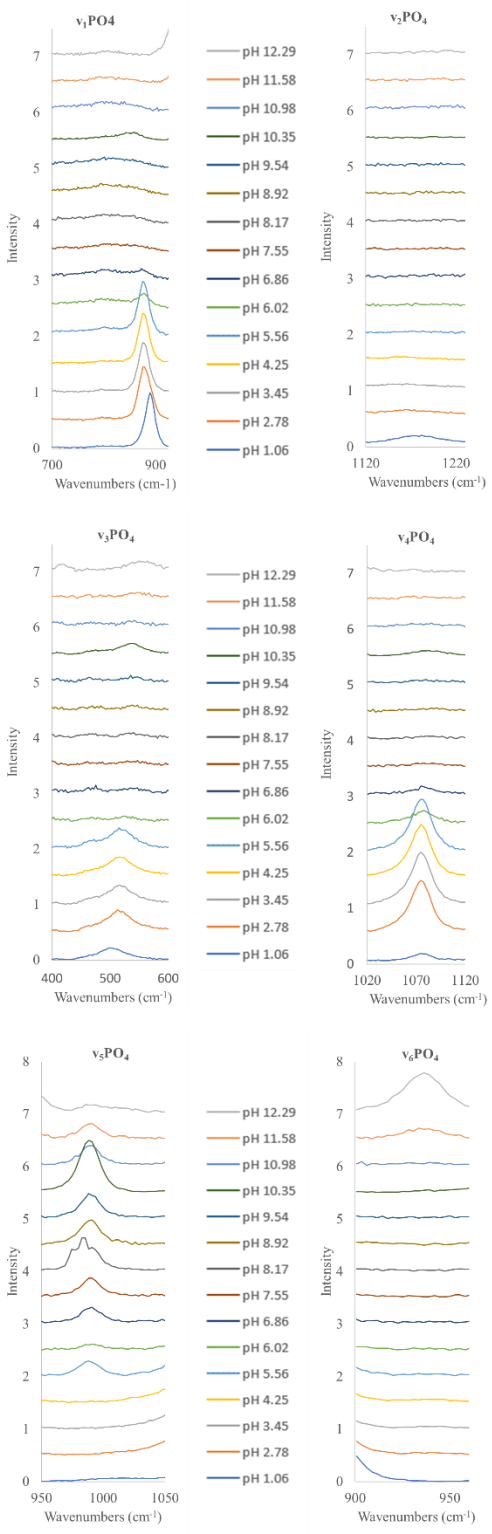

Figure 5) Raman spectra of individual phosphate peaks for NaH_2PO_4 mixed with HCl/NaOH at a range of pH's. Key: v_1: v_s{P(OH)3}; v_2: v{P=O}; v_3: δ_s{P(OH)3}; v_4: v_s{PO2}; v_5: v_{as}{P(OH)3} v_6: v_{as}{$P(OH)_2$} (v=stretching, δ=bending, s=symmetric, as=asymmetric) [6].

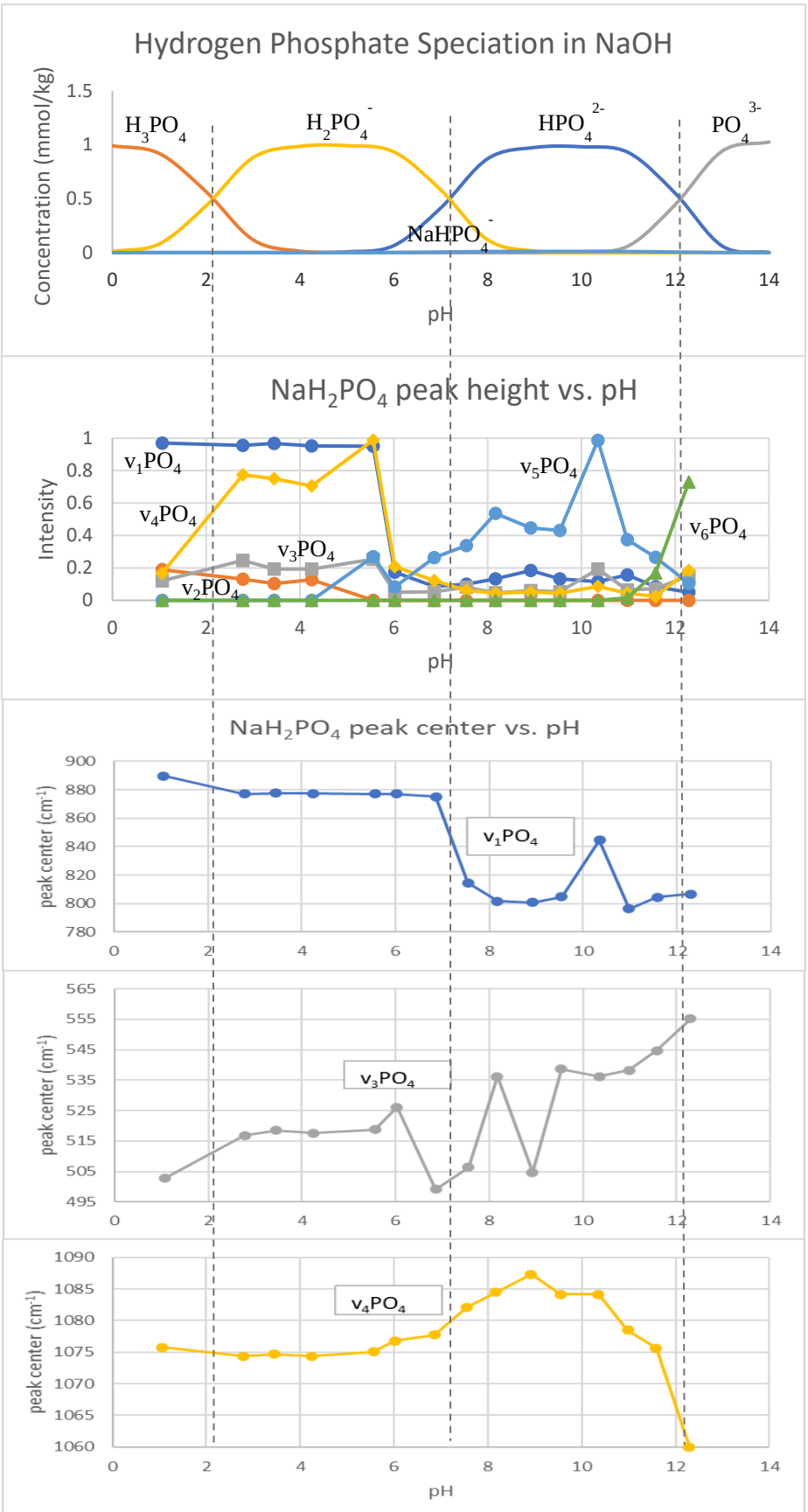
Hydrogen Phosphate Speciation in NaOH
Concentration (mmol/kg)
1.5
1
0.5
0
H3PO4
H2PO4-
HPO4 2-
PO4 3-
NaH2PO4-
0
2
4
6
8
10
12
14
pH
NaH2PO4 peak height vs. pH
Intensity
1
0.8
0.6
0.4
0.2
0
v1PO4
v4PO4
v3PO4
v2PO4
v5PO4
v6PO4
pH
NaH2PO4 peak center vs. pH
peak center (cm-1)
900
880
860
840
820
800
780
v1PO4
565
555
545
535
525
515
505
495
v3PO4
1090
1085
1080
1075
1070
1065
1060
v4PO4
pH

Figure 6) Phosphate speciation predicted by Geochemist's Workbench. 6b) Curve fit data for NaH_2PO_4 showing peak heights with respect to pH for the different phosphate vibrational frequencies. 6c) Curve fit data for NaH_2PO_4 showing peak centers with respect to pH for the different vibrational frequencies (Omitted the peaks that did not see a shift due to changing pH).

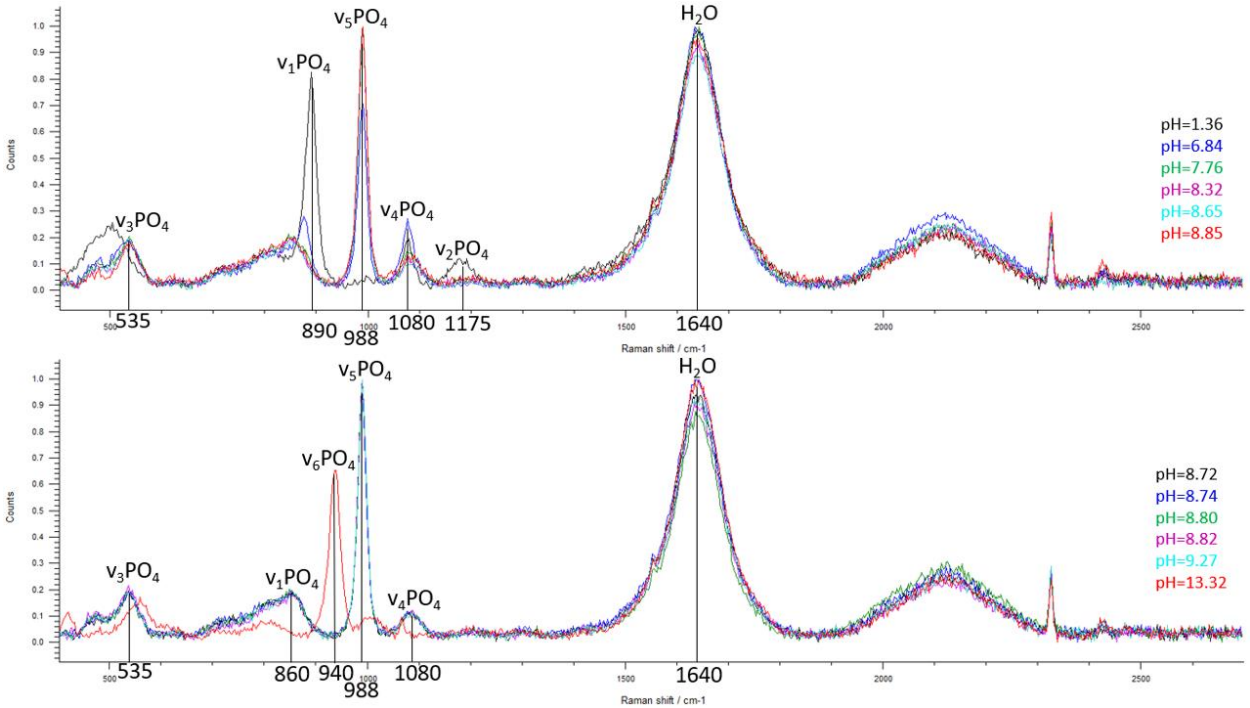

Figure 7a) Green laser spectra for Na_2HPO_4 brine mixed with the six different HCl buffers at various pH levels. 7b) Green laser spectra for Na_2HPO_4 brine mixed with the six different NaOH buffers at various pH levels.

Near saturated brine	HCl pH=0.1	HCl pH=1.0	HCl pH=1.95	HCl pH=2.99	HCl pH=4.04	HCl pH=5.01	UPW	NaOH pH=8.02	NaOH pH=8.99	NaOH pH=10.09	NaOH pH=11.02	NaOH pH=12.08	NaOH pH=12.98
H2O Sat NaCl	0.19	0.97	1.29	3.08	3.79	6.33	10.91	7.76	8.28	8.66	10.69	12.91	13.55
CaCl2	-0.63	-0.03	0.34	2.18	2.55	2.74	7.76	4.82	5.17	5.7	8.67	9.22	10.96
MgSO4	0.63	1.76	2.31	4.3	5.68	8.3	8.56	7.24	7.3	8.04	8.86	9.03	9.42
NaNO3	0.34	1.18	1.97	3.32	4.4	5.81	9.08	7.09	8.23	9.21	10.93	11.38	13.3
Na2SO4	0.88	2.01	2.75	4.02	4.9	5.17	9.9	6.91	8.21	8.33	11.05	13.31	14.23
MgCl2	-0.61	0.18	0.77	1.16	7.42	7.96	7.85	7.63	7.65	7.7	7.77	7.85	8.95
1M NaHCO3	5.15	9.17	9.86	9.87	9.89	10.23	9.9	9.56	9.65	9.72	9.8	9.81	13.35
0.1 mol/kg Na2CO3	0.59	1.67	9.59	10.82	10.85	10.86	10.63	10.67	10.69	10.72	10.75	10.91	13.52
NaHSO4	0.36	0.8	0.89	0.91	0.92	0.94	0.93	0.88	0.89	0.9	0.91	0.92	12.28
NH4Cl	0.39	1.23	1.92	3.44	3.86	4.48	6.31	5.65	5.74	5.82	7.21	8.68	9.67
NaF	2.28	4.67	5.21	6.34	6.58	6.68	10.46	7.38	7.5	10.61	10.96	11.23	13.32
NaClO4	0.29	1.08	1.7	1.78	3.44	3.84	4.37	6.35	6.55	9.58	9.83	11	13.38
NaClO3	0.31	1.14	1.72	1.75	3.49	3.63	4.28	5.78	6.18	6.41	9.66	9.9	13.36
NaH2PO4	1.06	2.78	3.45	4.25	4.3	4.33	4.27	4.25	4.28	4.35	4.54	5.56	10.35
Na2HPO4	1.36	6.84	7.76	8.32	8.65	8.85	8.56	8.72	8.74	8.8	8.82	9.27	13.32
H3PO4	0.64	1.07	1.21	1.24	1.26	1.28	1.27	1.18	1.2	1.23	1.59	1.85	4.96
UPW	0.58	1.34	2	4.17	4.41	6.91		7.88	8.4	8.9	11.2	11.39	12.57

Table 1. This matrix depicts all 16 brines and UPW mixed with the 6 HCl and 6 NaOH buffers and their corresponding pH values. Blue highlight shows the four samples analyzed in this paper that show significant changes in the Raman spectra with respect to pH changes. Yellow highlight shows the other samples with major spectral changes that will be analyzed in the near future. Non-highlighted samples show little to no changes within the Raman spectra with respect to pH changes and will not be of primary focus.

Works Cited

Benison, K. C., Goldstein, R. H., Wopenka, B., Burruss, R. C., & Pasteris, J. D. (1998). Extremely acid PERMIAN lakes and GROUND waters in North America. *Nature, 392*(6679), 911-914. doi:10.1038/31917

Benison, K. C., & Goldstein, R. H. (2002). Recognizing acid lakes and groundwaters in the rock record. *Sedimentary Geology*, *151*(3-4), 177–185. https://doi.org/10.1016/s0037-0738(02)00155-0

Ben Mabrouk, K., Kauffmann, T. H., Aroui, H., & Fontana, M. D. (2013). Raman study of cation effect on sulfate vibration modes in solid state and in Aqueous Solutions. *Journal of Raman Spectroscopy*, *44*(11), 1603–1608. https://doi.org/10.1002/jrs.4374

Clark, B. C., & Van Hart, D. C. (1981). The salts of Mars. *Icarus*, *45*(2), 370–378. https://doi.org/10.1016/0019-1035(81)90041-5

Dubessy, J., Boiron, M.-C., Moissette, A., Monnin, C., & Sretenskaya, N. (1992). Determinations of water, hydrates and ph in fluid inclusions by micro-raman spectrometry. *European Journal of Mineralogy*, *4*(5), 885–894. https://doi.org/10.1127/ejm/4/5/0885

Elwood Madden, M. E., Madden, A. S., Rimstidt, J. D., Zahrai, S., Kendall, M. R., & Miller, M. A. (2012). Jarosite dissolution rates and Nanoscale mineralogy. *Geochimica Et Cosmochimica Acta*, *91*, 306–321. https://doi.org/10.1016/j.gca.2012.05.001

Hinkel, N. R., Hartnett, H. E., & Young, P. A. (2020). The influence of stellar phosphorus on our understanding of exoplanets and astrobiology. *The Astrophysical Journal*, *900*(2). https://doi.org/10.3847/2041-8213/abb3cb

Howard, A. A., Tschumper, G. S., & Hammer, N. I. (2010). Effects of hydrogen bonding on vibrational normal modes of pyrimidine. *The Journal of Physical Chemistry A*, *114*(25), 6803–6810. https://doi.org/10.1021/jp101267w

Hurowitz, J. A., Grotzinger, J. P., Fischer, W. W., McLennan, S. M., Milliken, R. E., Stein, N., Vasavada, A. R., Blake, D. F., Dehouck, E., Eigenbrode, J. L., Fairén, A. G., Frydenvang, J., Gellert, R., Grant, J. A., Gupta, S., Herkenhoff, K. E., Ming, D. W., Rampe, E. B., Schmidt, M. E., … Wiens, R. C. (2017). Redox stratification of an ancient lake in Gale CRATER, MARS. *Science*, *356*(6341). https://doi.org/10.1126/science.aah6849

Kneipp, K., Kneipp, H., Itzkan, I., Dasari, R. R., & Feld, M. S. (1999). Ultrasensitive chemical analysis BY Raman spectroscopy. *Chemical Reviews*, *99*(10), 2957–2976. https://doi.org/10.1021/cr980133r

Lauro, S. E., Pettinelli, E., Caprarelli, G., Guallini, L., Rossi, A. P., Mattei, E., Cosciotti, B., Cicchetti, A., Soldovieri, F., Cartacci, M., Di Paolo, F., Noschese, R., & Orosei, R. (2021). Multiple subglacial water bodies below the South Pole of Mars unveiled by New Marsis Data. *Nature Astronomy*, *5*(1), 63–70. https://doi.org/10.1038/s41550-020-1200-6

McEwen, A. S., Dundas, C. M., Mattson, S. S., Toigo, A. D., Ojha, L., Wray, J. J., Chojnacki, M., Byrne, S., Murchie, S. L., & Thomas, N. (2013). Recurring slope lineae in equatorial regions of Mars. *Nature Geoscience*, *7*(1), 53–58. https://doi.org/10.1038/ngeo2014

McGraw, L. E., McCollom, N. D., Phillips-Lander, C. M., & Elwood Madden, M. E. (2018). Measuring perchlorate and sulfate in planetary brines Using Raman spectroscopy. *ACS Earth and Space Chemistry, 2*(10), 1068-1074. doi:10.1021/acsearthspacechem.8b00082

Michalski, J. R., Cuadros, J., Niles, P. B., Parnell, J., Deanne Rogers, A., & Wright, S. P. (2013). Groundwater activity on Mars and implications for a DEEP biosphere. *Nature Geoscience*, *6*(2), 133–138. https://doi.org/10.1038/ngeo1706

Ojha, L., Wilhelm, M. B., Murchie, S. L., McEwen, A. S., Wray, J. J., Hanley, J., Massé, M., & Chojnacki, M. (2015). Spectral evidence for hydrated salts in recurring slope lineae on Mars. *Nature Geoscience*, *8*(11), 829–832. https://doi.org/10.1038/ngeo2546

Pritchett, B. N., Elwood Madden, M. E., & Madden, A. S. (2012). Jarosite dissolution rates and maximum lifetimes in high SALINITY Brines: Implications for Earth and Mars. *Earth and Planetary Science Letters*, *357-358*, 327–336. https://doi.org/10.1016/j.epsl.2012.09.011

Sapers, H. M., Razzell Hollis, J., Bhartia, R., Beegle, L. W., Orphan, V. J., & Amend, J. P. (2019). *The cell and the sum of its parts: Patterns of complexity in biosignatures as revealed by deep UV Raman spectroscopy*. Frontiers in microbiology, Vol.10, p.679-679. https://www.frontiersin.org/articles/10.3389/fmicb.2019.00679/full.

Sharma, S. K., Porter, J. N., Misra, A. K., Acosta-Maeda, T. E., Angel, S. M., & McKay, C. P. (2020). Standoff Raman spectroscopy for Future Europa lander missions. *Journal of Raman Spectroscopy*, *51*(9), 1782–1793. https://doi.org/10.1002/jrs.5814

Shende, C., Farquharson, S., Farquharson, D., & Brouillette, C. (2021). Measurements of bicarbonate in water containing ocean-level sulfate using a simple multi-pass optical raman system. *Oceans*, *2*(2), 330–336. https://doi.org/10.3390/oceans2020019

Squyres, S. W., Grotzinger, J. P., Arvidson, R. E., Bell, J. F., Calvin, W., Christensen, P. R., Clark, B. C., Crisp, J. A., Farrand, W. H., Herkenhoff, K. E., Johnson, J. R., Klingelhöfer, G., Knoll, A. H., McLennan, S. M., McSween, H. Y., Morris, R. V., Rice, J. W., Rieder, R., & Soderblom, L. A. (2004). In situ evidence for an Ancient aqueous environment at Meridiani Planum, Mars. *Science*, *306*(5702), 1709–1714. https://doi.org/10.1126/science.1104559

Uckert, K., Bhartia, R., Beegle, L. W., Monacelli, B., Asher, S. A., Burton, A. S., Bykov, S. V., Davis, K., Fries, M. D., Jakubek, R. S., Hollis, J. R., Roppel, R. D., & Wu, Y.-H. (2021). Calibration of the sherloc deep ultraviolet fluorescence–raman spectrometer on the perseverance rover. *Applied Spectroscopy*, 000370282110133. https://doi.org/10.1177/00037028211013368